ARR No. E5B01

NATIONAL ADVISORY COMMITTEE FOR AERONAUTICS

WARTIME REPORT

ORIGINALLY ISSUED

February 1945 as
Advance Restricted Report E5B01

MEASUREMENT OF OPERATING STRESSES IN AN AIRCRAFT ENGINE CRANKSHAFT UNDER POWER

By Douglas P. Walstrom

Aircraft Engine Research Laboratory
Cleveland, Ohio

NACA

WASHINGTON

NACA ARR No. E5B01

NATIONAL ADVISORY COMMITTEE FOR AERONAUTICS

ADVANCE RESTRICTED REPORT

MEASUREMENT OF OPERATING STRESSES IN AN AIRCRAFT ENGINE CRANKSHAFT UNDER POWER

By Douglas P. Walstrom

SUMMARY

Strain-gage measurements were made on the crankshaft of a Wright R-1820-73 test engine while under power. Bakelite-bonded wire strain gages were installed on the front half of the crankshaft and the connecting wires were brought out through the oil passages and connected to slip rings at the rear of the engine.

Bending and tensile-compressive strains at various sections in the web were measured by pairs of strain gages and strains at several points on the front half of the crankshaft were measured by single strain gages. Peak stresses were determined from oscillograph records and the harmonic components of stress were determined by a wave analyzer.

Strains were measured with the engine being driven by the dynamometer at a range of speeds and also with the engine operating under power at a range of speeds and powers. A harmonic analysis of the gas pressures in the cylinder was made at constant speed and a range of powers.

Results showed that the inertia-excited stresses varied almost directly with speed and that the stresses caused by gas-pressure forces varied with the indicated mean effective pressure. When the engine operated under severe knock, observations showed no change in crankshaft stresses. No direct relation was found between stresses in the crankshaft and the torsional-vibration amplitudes as determined by a torsiograph installed at the rear of the crankshaft. Strain-gage measurements on an aircraft-engine crankshaft in flight or in an engine-propeller test stand are believed to be practicable.

INTRODUCTION

The determination of operating stresses in an aircraft-engine crankshaft under power would be of value in crankshaft development because it would supplement theoretical calculations and laboratory tests. Bakelite-bonded strain gages applied to the accessible parts of the operating crankshaft, with connecting wires brought out through the oil passages, make possible the following:

1. Measurement of actual peak stresses

2. Separation of stresses into bending, torsional, and tensile stresses

3. Analysis of the forces applied to the crankshaft

Curtis (reference 1) applied strain gages to the crankshaft of a stationary Diesel engine. As the result of strain measurements in the crankweb, he was able to explain a series of breakages and to show that installation of torsional-vibration dampers reduced the strains to a safe value.

The tests reported herein give the results of strain-gage measurements made at the NACA Cleveland laboratory during the summer of 1944 on the crankshaft of a Wright R-1820-73 (C9GC) test engine over a range of operating conditions. The technique of strain-gage measurement and the accessory apparatus used is described. Data are given on bending and tensile-compressive stresses at various sections of the web and on stresses at several points on the front half of the crankshaft. Alternating stresses only were measured.

The two types of exciting force, inertia and gas pressure, were separately analyzed. Stresses caused by inertia forces were determined by driving the engine with the dynamometer and the gas-pressure forces were qualitatively determined with a pressure indicator. The engine was operated under power (the condition where both inertia and gas-pressure forces are present) at a range of speeds and manifold pressures and the stresses were measured. In order to determine whether knock produced any stresses in the crankshaft, the engine was operated under severe knock. Torsional-vibration measurements were made to supplement the stress measurements.

APPARATUS

Tests were conducted on a Wright R-1820-73 engine converted for test purposes. Cylinder 1 was operated under power; cylinders 4 and 7 were operated without firing for balance with pistons,

connecting rods, and valves in place but without push rods. The other cylinders were removed. The propeller reduction gears were replaced with a direct connection and the pendulum dampers were replaced with rigidly attached counterweights. The supercharger impeller and gearing were removed. Auxiliary equipment used for controlling and measuring engine conditions is shown in figure 1.

Thirteen strain gages were installed on the front half of the crankshaft and connecting wires were brought out of the engine as shown in figure 2. The wires, No. 32 enameled double cotton covered, were attached to the surface of the crankshaft with Bakelite cement, BC-6035, up to where they passed through an oiltight neoprene packing into the drilled oil passage. The wires were twisted together and covered with a flexible braided-glass sleeving. A hollow extension shaft was attached to the starter-shaft coupling. The shaft contained a second neoprene oil seal that allowed the wires to pass through to where they were connected to the slip rings. At the disassembly of the engine after 300 hours' operation, this installation of connecting wires and oil seals was found to be in good condition.

The slip-ring device (ordinarily called a "pineapple"), which was attached to the extension shaft, consisted of a set of 12 monel slip rings mounted on a spindle rotating with the shaft and a stationary outer case supported by bearings to allow relative rotation. This outer case supported the silver-graphite brushes, 1/8 inch in diameter, which were held against the slip rings by small helical springs. Two brushes, 180° apart, were used for each ring. A timing device contained in the pineapple generated a sharp electrical impulse at each revolution of the shaft. A view of the pineapple installed on the engine is shown in figure 3.

Individually shielded wires connected the pineapple to a terminal box containing load resistors, switches, and terminals. Connections could be made from this terminal box to the wave analyzer, the cathode-ray oscilloscope, or to the 12-channel amplifier and recording oscillograph. Provision was made for applying a calibrating voltage of known magnitude to each channel of the amplifier.

A magnetostriction-type pressure indicator was installed in a tapped hole in the cylinder and connected to the terminal box.

STRAIN-MEASUREMENT TECHNIQUE

Construction and Application of Strain Gages

Strain gages suitable for aircraft-engine application must be resistant to high temperature and engine oil. A bakelite-bonded

resistance-type electric strain gage fulfilling these requirements has been developed by the NACA. (See reference 2.) This type of strain gage can be used at temperatures up to 500° F, is unaffected by engine oil, and is rugged and durable. Some of the strain gages used in this investigation were made by the NACA, using Advance wire. The other gages were bakelite-bonded strain gages commercially manfactured, using Iso-Elastic wire. (See table in fig. 4.)

The strain gages were attached with Bakelite cement, BC-6035, and the entire assembly was baked in an oven. The connecting wires were attached to the crankshaft with Bakelite cement at the same time.

Gage Constant

When a resistance-type strain gage is cemented to a test object, the component of strain in the test material in the direction of the gage axis produces a change in the electrical resistance of the strain gage. This change in resistance has been found to be a linear function of the strain within the elastic limit of the test material. The ratio of unit change in strain-gage resistance to unit strain in the member is defined as the gage constant and may be expressed as

$$\frac{\Delta R}{R} = k \times \epsilon \qquad (1)$$

where

ΔR change in strain-gage resistance, ohms

R resistance of strain gage, ohms

k gage constant

ϵ strain in material at surface, inches per inch

The value of k depends upon the material used for the gage-resistance wire.

Basic Strain-Gage Circuit for Single Strain Gage

The basic circuit for measurements with a single strain gage is shown in figure 5(a). The strain gage is R_g; R_d is a load resistor that is approximately equal to R_g. Under the conditions of zero strain, the voltage drop e across the strain gage is

$$e = E_B \frac{R_g}{R_g + R_d}$$

where

E_B battery voltage

Under strain the gage resistance changes by an amount ΔR and the voltage across the strain gage becomes

$$e' = E_B \frac{R_g + \Delta R}{R_g + \Delta R + R_d}$$

In the measurement of vibratory strains, this circuit is coupled to the amplifying or measuring circuit with a condenser that blocks off the direct component of battery voltage. The alternating component of battery voltage across the gage is

$$E_{ac} = e' - e$$

$$= E_B\left(\frac{R_g + \Delta R}{R_g + \Delta R + R_d} - \frac{R_g}{R_g + R_d}\right)$$

$$= E_B\left[\frac{\Delta R \times R_d}{R_g^2 + R_d^2 + 2R_dR_g + \Delta R(R_d + R_g)}\right]$$

where

E_{ac} alternating component of battery voltage, peak volts

Inasmuch as ΔR in practice is very small compared with R_g and R_d, the last term in the denominator may be dropped with negligible error. When it is assumed that $R_d = a \times R_g$, the result is

$$E_{ac} = \frac{E_B \Delta R}{R_g} \times \frac{a}{(1 + a)^2}$$

Substituting from equation (1) and rearranging

$$\text{strain} = \frac{E_{ac}}{E_B k} \times \frac{(1 + a)^2}{a} \qquad (2)$$

In the case where $R_d = R_g$, then $a = 1$ and the expression becomes

$$\text{strain} = \frac{4E_{ac}}{E_B k} \qquad (3)$$

The stress (lb/sq in.) is found by substituting the proper value of modulus of elasticity E (lb/sq in.) for the test material,

$$\text{stress} = \frac{4E\,E_{ac}}{E_B k} \tag{4}$$

Measurement of Bending Strains

For the measurement of bending strains, a pair of similar strain gages is applied to the test member back to back as shown in figure 5(d) and connected as shown in figure 5(b). No load resistor is required. When a bending load is applied to the test member, the top strain gage is in tension and increases in resistance, whereas the bottom strain gage is in compression and decreases in resistance. If another load, such as a tensile load, is applied in addition to the bending, each strain gage will increase in resistance an equal amount with a cancelation of effect. The circuit is therefore sensitive only to bending strains. When the same kind of derivation is used for this circuit as is used for the single strain gage, the expression for bending strain can be shown to be

$$\text{strain} = \frac{2E_{ac}}{E_B k} \tag{5}$$

It should be noted that the sensitivity obtained is twice that of the single strain-gage case of equation (3); that is, with equal battery voltage, gage constant, and strain, twice the output voltage is produced.

Measurement of Tensile-Compressive Strains

For the measurement of tensile-compressive strains, a pair of similar strain gages is applied to the test member back to back as shown in figure 5(e) and connected as in figure 5(c). The load resistor R_d is usually made equal to the sum of the two strain gages R_{g_1} and R_{g_2}. When a pure tensile or compressive load is applied to the test member, each strain gage equally increases or decreases in resistance. If an additional load, such as a bending load, is applied to the test member, one strain gage will increase in resistance and the other will decrease in resistance by the same amount, with a cancelation of effect. The arrangement therefore is sensitive only to tensile-compressive strains. If R_{g_1} and R_{g_2} are similar and if it is assumed that $R_d = a\left(R_{g_1} + R_{g_2}\right)$, the expression for strain can be shown to be

$$\text{strain} = \frac{E_{ac}(1 + a)^2}{E_B k a} \tag{6}$$

and when $\left(R_{g_1} + R_{g_2}\right) = R_d$, the expression is

$$\text{strain} = \frac{4E_{ac}}{E_B k} \tag{7}$$

The sensitivity of this combination is the same as for a single strain gage.

Forces and Moments on Crankshaft

The force exerted on the crankpin may be resolved into four components in the crankweb as shown in figures 6(b) to 6(e). The reaction of the counterweights produces additional forces. Pairs of strain gages were located to measure separately strains resulting from components (b) and (d) of figure 6, as shown by figure 7. Components (c) and (e) of figure 6 can also be measured by strain gages if desired. Gage 11 was applied to measure strains in the fillet and gage 12 was applied to measure strains in the cheek near the counterweight. The combined circuit for all the strain gages is shown in figure 4.

Determination of Stresses

The use of a 12-channel amplifier and recording oscillograph makes possible the recording of several strain records, a cylinder-pressure record, and a timing trace. These simultaneous records facilitate the interpretation of forces. The 12 amplifiers operate at constant amplification and each includes an input attenuator that can be set to give a known ratio between input voltage to the attenuator and the voltage applied to the amplifier.

In order to calibrate the system, an alternating voltage of known amount is applied to the input of all channels at a certain attenuator setting and an oscillograph record is made. Records of the strain signals under test conditions are then made, the attenuator setting being carefully noted. Inasmuch as the height of trace produced by the known voltage at a known attenuation and the height of trace of the unknown strain signal at a known attenuation is established, the alternating strain voltage E_{ac} can be determined. When alternating strain voltage, strain-gage constant,

battery voltage, and modulus of elasticity are substituted in the proper formula, the stress is obtained. An accuracy of ±5 percent in the determination of stress is believed possible.

The wave analyzer was used to analyze the harmonic components of the complex-wave form of the strain signals and gave the value of E_{ac} for each component in rms volts.

Slip-Ring Interference

A serious factor in wire-strain-gage measurements on rotating members is the variation of resistance caused by slip rings in the circuit in series with the strain gage. If the strains are small, this variation appearing as an IR drop might be of the same order as the strain-gage signal and will cause error in the measurements. It is possible, however, to obtain satisfactory results if brushes and slip rings are operating correctly. The data in this report were taken using the series type of circuit shown in figure 4.

Some of the measurements were repeated with the strain gages connected in a Wheatstone bridge arrangement. The results were in agreement and it was found that the bridge connection practically eliminated the slip-ring interference. Figure 5(f) shows the basic bridge circuit of a pair of gages and figure 5(g) shows a combination of circuits on a rotating member. The circuits are supplied by a common battery. Resistors R_1, R_2, and R_d are mounted on the rotating shaft. The condensers serve to bypass the high-frequency components of the interference. The added complications of the bridge circuit are a disadvantage.

TEST PROCEDURE

In the tests reported herein, inertia forces were determined by driving the engine with the dynamometer at a range of speeds, making oscillograph records, and taking wave-analyzer readings at several points. Peak stresses were determined from oscillograph records as previously described and the harmonic components of stress (expressed as multiples of crankshaft speed) were calculated from wave-analyzer data.

In order to determine the exciting forces caused by gas pressure, the pressure-indicator output was analyzed for the various harmonic components of cylinder pressure with the engine under power.

Strains produced by the combination of inertia and gas-pressure forces were determined with the engine operating at constant power (imep, 227 lb/sq in.) and a range of speeds. Oscillograph and wave-analyzer data were taken of the strain signals.

The engine was then operated at constant speed and a range of manifold pressures. The variation of the harmonic components of cylinder pressure with manifold pressure was determined by wave analysis of the pressure-indicator output and the variation in crankshaft stresses were determined by oscillograph and wave-analyzer data.

The engine was operated under severe knocking conditions at an engine speed of 2400 rpm to investigate the possible effect of knock on crankshaft stresses. The strain-gage signals were carefully observed, one at a time, on a cathode-ray oscilloscope screen and oscillograph records were made for further study.

A torsiograph was installed on the rear extension shaft in place of the pineapple and oscillograph and wave-analyzer data were taken at normal rated power (imep, 227 lb/sq in.) over a range of speeds.

All tests were conducted under the following engine conditions:

Oil-in temperature, $^{\circ}F$	160
Temperature of rear spark-plug bushing (maximum), $^{\circ}F$	450
Combustion-air temperature (except for knock test), $^{\circ}F$	95
Fuel-air ratio	0.095

The fuel used was 100 octane.

RESULTS AND DISCUSSION

Typical oscillograph records taken during the various tests are shown in figures 8 to 13. The records have been retraced by hand in the reproduction process.

Some representative curves showing the bending stresses caused by inertia forces are shown in figure 14. An arbitrary straight line has been drawn through the peak-stress points to represent their increase with speed. It can be noted that a large third-order stress is present. Other harmonics were found in addition to those plotted. A value of $E = 30 \times 10^6$ pounds per square inch was assumed in the stress calculations. Two typical oscillograph records taken with the engine being motored are shown in figures 8 and 9.

Results of the harmonic analysis of gas pressure in the cylinder are plotted in figure 15. It can be seen that there is a harmonic component of gas pressure at each order and half order, successively decreasing in amplitude. Half orders higher than $3\frac{1}{2}$ were not determined. Orders and half orders higher than 9 were found but were too small for dependable measurement. The same results were obtained at different speeds. This figure is similar to that given by Lürenbaum (reference 3). The dashed lines show components of cylinder pressures while the engine was being motored; the inertia forces therefore include the forces caused by the pumping action. The actual cylinder pressures were not determined.

With the engine operating under power, the alternating strains result from the combined inertia and gas-pressure forces. Curves of the peak stress and of the important harmonic components are plotted in figures 16 and 17 for bending and tensile-compressive stresses, respectively. A comparison of figure 16 with figure 14 shows that the half- and first-order harmonics have increased in magnitude but that the third-order harmonic has decreased somewhat. This decrease may be explained by the fact that the gas-pressure-excited third-order component apparently acts in phase opposition to the larger inertia-excited third order. It can be noted from figure 17 that the third-order harmonic of tensile-compressive stress is the largest of the harmonics. From figures 16 and 17 it can be noted that the inertia-excited stresses form a large part of the total stresses. The large third-order component is undoubtedly characteristic of the three-cylinder test engine and would not be expected in the regular nine-cylinder engine.

Figures 10, 11, and 12 show oscillograph records of strain signals taken while the engine was under power. It can be seen that the peak stresses increase with both speed and manifold pressure.

A simultaneous record of several strain signals is presented in figure 18. A careful study and comparison of the various traces reveals information on the nature of the forces applied to the crankshaft, such as:

1. The peak in the bending stress from strain gages 2 and 3 coincides with the maximum cylinder pressure.

2. The tensile-compressive stresses from strain gages 4 and 5 resemble those from strain gages 6 and 7 but are opposite in direction.

3. Stresses of appreciable magnitude are shown by strain gage 12 located near one of the counterweights. In the regular engine with the pendulum dampers, information on the forces exerted on the crankshaft by the dampers may be gained by similar strain measurements near the damper holes.

Strain gages 8 and 9 and strain gage 11 produced signals too small for dependable measurement and were disconnected.

A plot of relative pressures against mean effective pressure (fig. 19) indicates that each harmonic component of the cylinder pressure increases with manifold pressure. These results are similar to those shown in reference 4. The increase in gas-pressure exciting forces results in increased bending and tensile-compressive stresses as shown in figure 20. The exception here again is the strong, inertia-excited third order.

Careful observation failed to show any effect of knock in the strain-gage signals even under severe knocking conditions. This observation is in agreement with the theoretical analysis of Geiger (reference 5).

Curves of the peak torsional-vibration amplitudes and of the main harmonic components are shown in figure 21 and a typical oscillograph record is shown in figure 13. The hump in the first-order harmonic in figure 21 at an engine speed of 2100 rpm is believed to be caused by a resonance in the crankshaft-flywheel-dynamometer system of the test engine. A comparison of the torsional-vibration amplitudes with the stresses shown in figures 16 and 17 shows no direct relation. The first-order peak is not present in the stress curves and the prominent third-order stress is not apparent in the torsional vibrations.

SUMMARY OF RESULTS

From an investigation of the measurement of operating stresses in an aircraft-engine crankshaft under power, the following results were obtained:

1. Inertia-excited bending and tensile-compressive stresses increase almost directly with speed.

2. A large inertia-excited third-order stress was found in both the bending and tensile-compressive cases. This excitation is a characteristic of the three-cylinder test engine.

3. Harmonics of cylinder gas pressure of appreciable magnitude were found for each order and half order up to 9.

4. The peak in the bending stress in the web coincides with the maximum cylinder pressure.

5. Each harmonic of cylinder gas pressure was found to increase almost directly with manifold pressure. The measured stresses increased in similar fashion.

6. No effect of knock on the crankshaft stresses was noted.

7. The torsional-vibration amplitudes at the rear of the engine were not directly related to the stresses in the crankshaft.

CONCLUDING REMARKS

1. The results presented demonstrate the practicability of making direct strain measurements on a crankshaft under operating conditions.

2. Strain measurements on an engine crankshaft, either in flight or in a propeller test stand, may be made. The application of strain gages requires only minor alterations and the mounting of the pineapple in place of the starter is not a serious problem. Amplifying and recording instruments for flight use are available.

3. Most of the radial aircraft engines now in use have a hollow shaft coupled to the crankshaft accessible at the rear of the engine and are well suited to a strain-gage installation. Such an installation on an in-line engine would be more difficult.

Aircraft Engine Research Laboratory,
National Advisory Committee for Aeronautics,
Cleveland, Ohio.

REFERENCES

1. Curtis, W. F.: Dynamic Strain Measurements in the Crankshaft of a Diesel Engine. Rep. R-154, Bur. Ships, Navy Dept., Oct. 1943.

2. Nettles, J. Cary, and Tucker, Maurice: Construction of Wire Strain Gages for Engine Application. NACA ARR No. 3L03, 1943.

3. Lürenbaum, Karl: Vibration of Crankshaft-Propeller Systems. SAE Jour. (Trans.), vol. 39, no. 6, Dec. 1936, pp. 469-478.

4. Wilson, W. Ker: Practical Solution of Torsional Vibration Problems. Vol. 1. John Wiley & Sons, Inc., 2d ed., 1940, pp. 452-456.

5. Geiger, J.: Engine Stresses Induced by Rapid Pressure Rise and Fuel Knock. (From Auto. tech. Zeitschr., Jahrg. 44, Nr. 13, July 10, 1941, pp. 327-335.) R.T.P. Trans. No. 1433, Ministry of Aircraft Prod. (British).

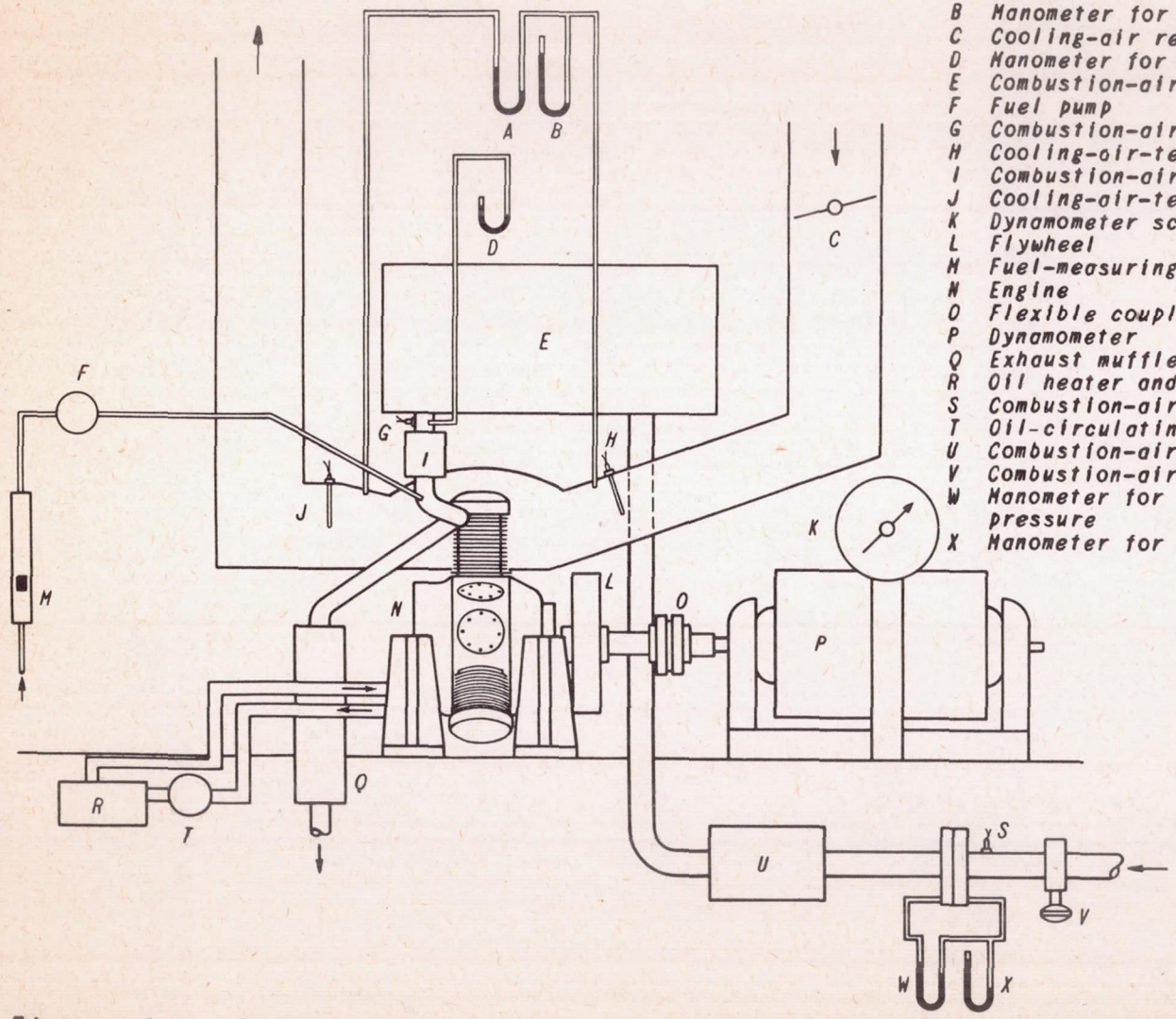

A Manometer for cooling-air pressure drop
B Manometer for cooling-air pressure (upstream)
C Cooling-air regulator
D Manometer for manifold pressure
E Combustion-air surge tank
F Fuel pump
G Combustion-air-temperature thermocouple
H Cooling-air-temperature thermocouple (upstream)
I Combustion-air filter
J Cooling-air-temperature thermocouple (downstream)
K Dynamometer scales
L Flywheel
M Fuel-measuring rotameter
N Engine
O Flexible coupling
P Dynamometer
Q Exhaust muffler
R Oil heater and cooler
S Combustion-air-temperature thermocouple
T Oil-circulating pump
U Combustion-air heater
V Combustion-air-pressure regulator
W Manometer for combustion-air-orifice differential pressure
X Manometer for combustion-air pressure (upstream)

NATIONAL ADVISORY
COMMITTEE FOR AERONAUTICS

Fig. 1

Figure 1. - Diagrammatic sketch of test engine and auxiliary equipment.

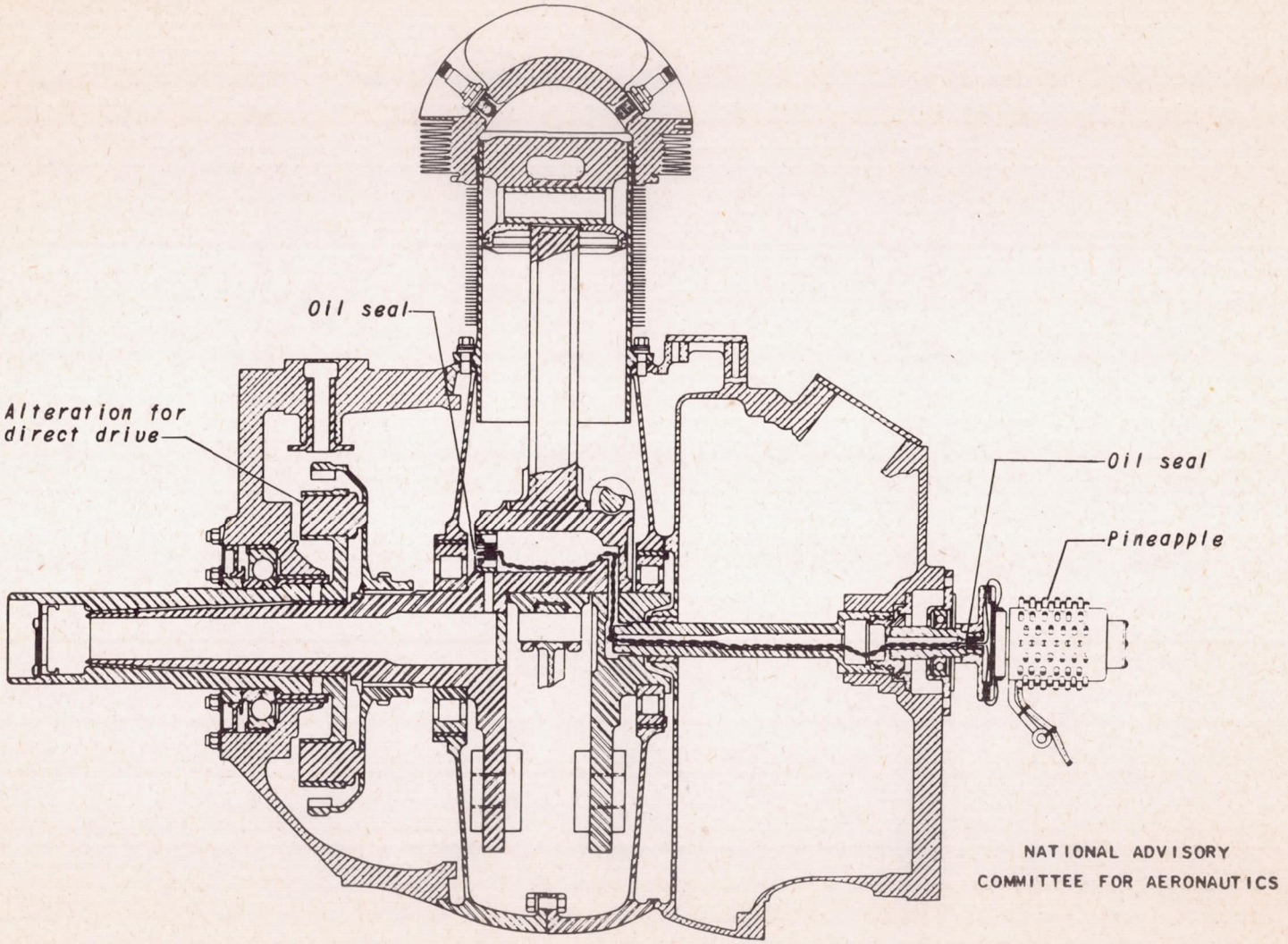

Figure 2. - Simplified cross section of test engine showing method of bringing out wires.

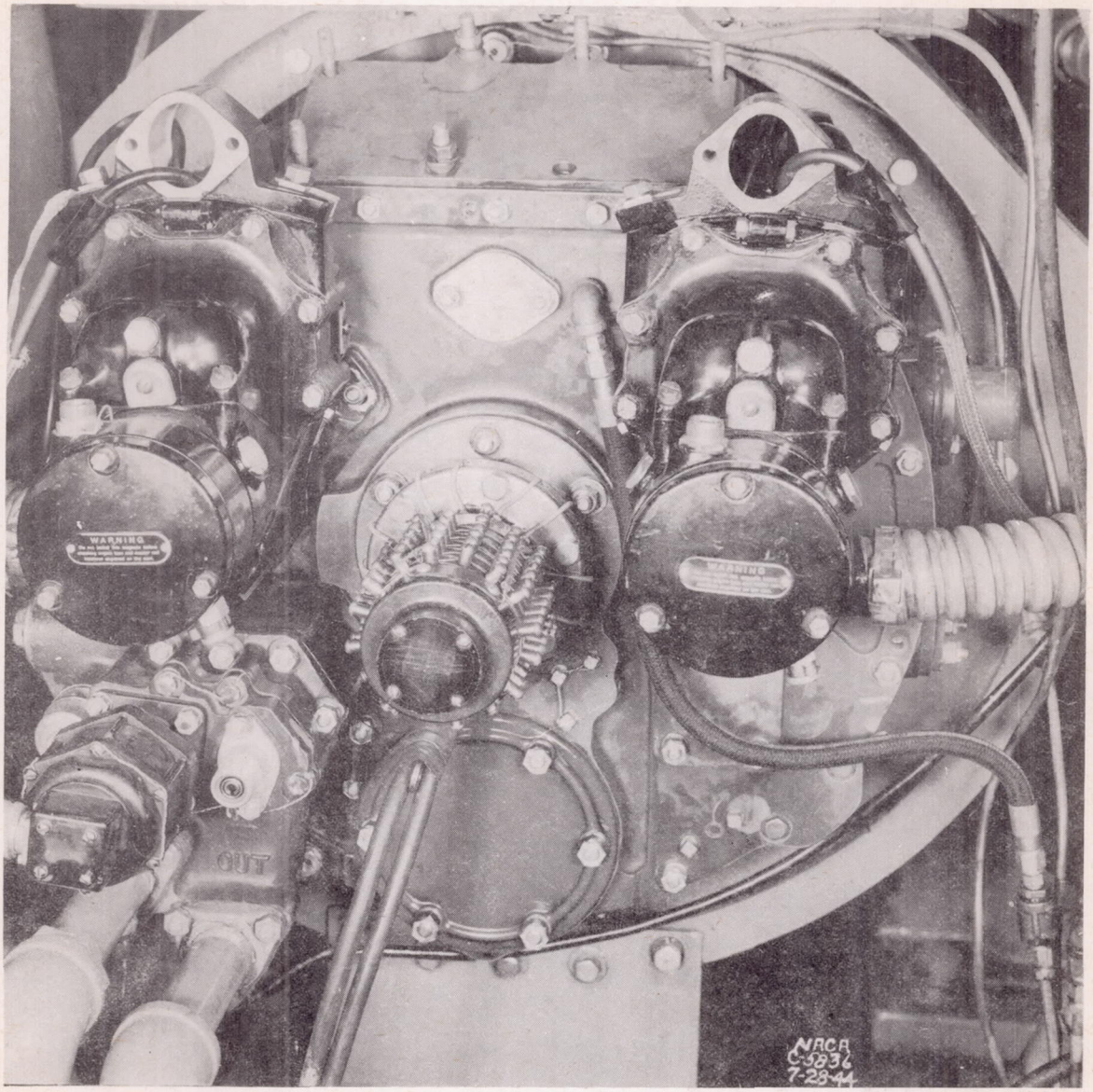

Figure 3. - Pineapple installation at rear of engine.

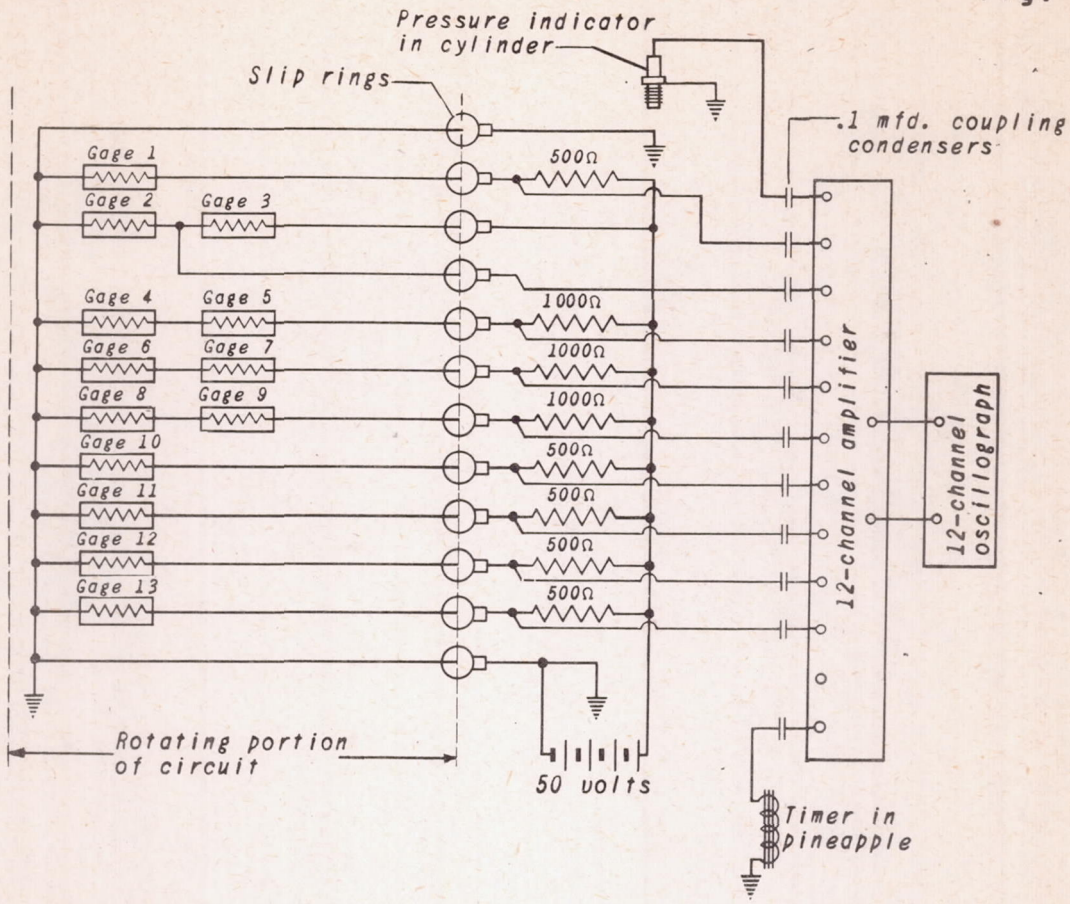

Gage	Function	Resistance (ohms)	Strain gage constant, K	Strain gage wire	Strain gage length (in.)
1	Single	425	2.00	Advance	1/2
2 and 3	Bending	498	3.43	Iso-Elastic	1/4
4 and 5	Tensile-compressive	505	3.43	Iso-Elastic	1/4
6 and 7	Tensile-compressive	503	3.43	Iso-Elastic	1/4
8 and 9	Tensile-compressive	408	2.00	Advance	1/2
10	Single	392	2.00	Advance	1/2
11	Single	210	2.00	Advance	1/4
12	Single	400	2.00	Advance	1/2
13	Single	210	2.00	Advance	1/4

NATIONAL ADVISORY
COMMITTEE FOR AERONAUTICS

Figure 4. - Combined circuit for all strain gages.

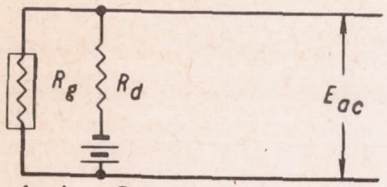

(a) Basic circuit for single strain gage.

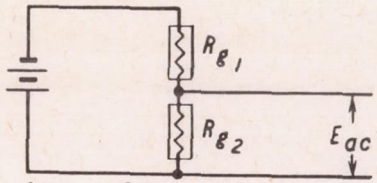

(b) Circuit using pair of strain gages for bending measurements.

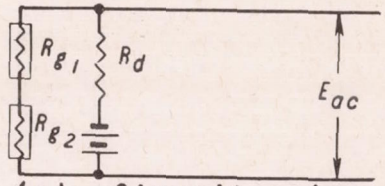

(c) Circuit using pair of strain gages for tensile-compressive measurements.

(d) Pair of strain gages applied for bending measurements.

(e) Pair of strain gages applied for tensile-compressive measurements.

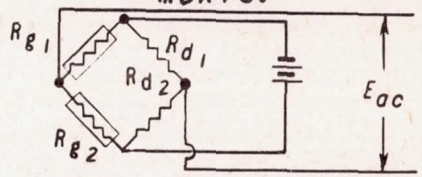

(f) Wheatstone bridge connection for bending measurements.

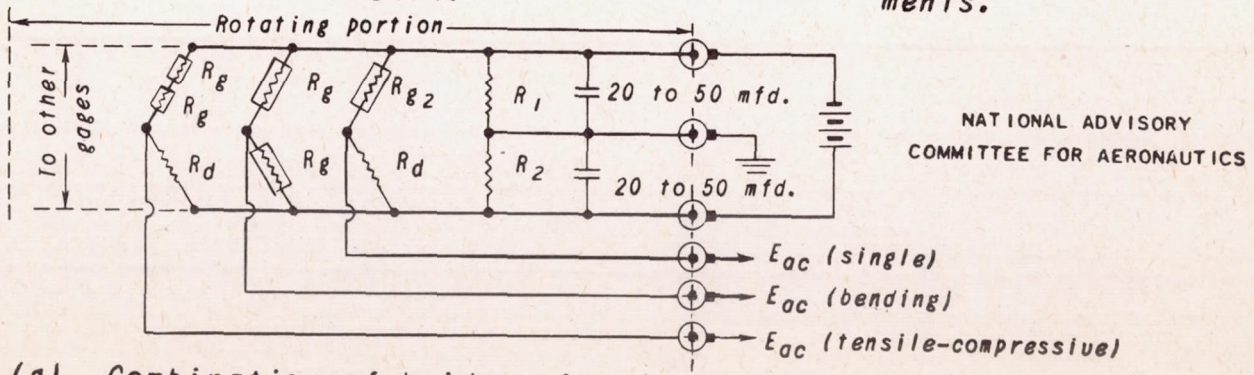

NATIONAL ADVISORY COMMITTEE FOR AERONAUTICS

(g) Combination of bridge circuits on rotating member.

Figure 5. - Strain gage applications.

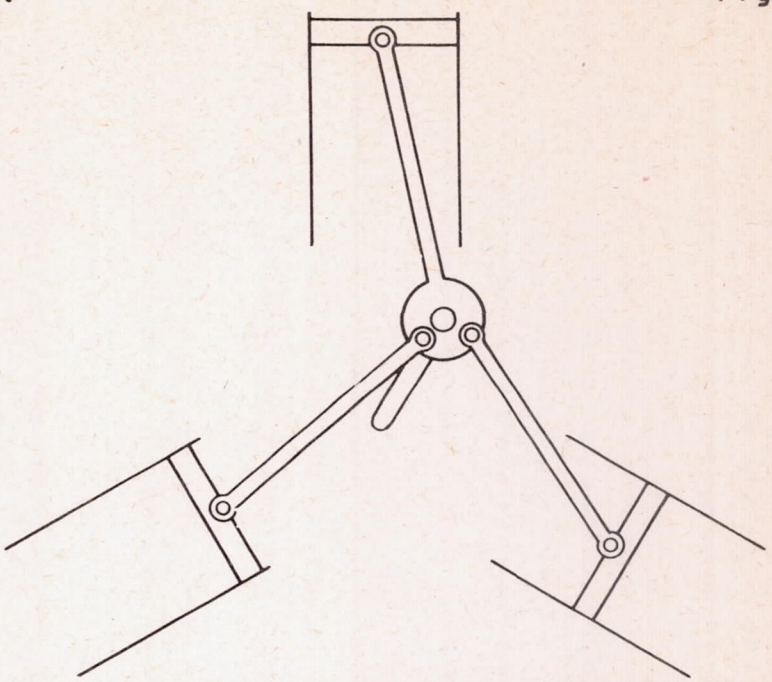

(a) Three-cylinder test engine.

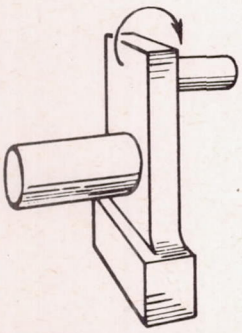

(b) Bending moment normal to web.

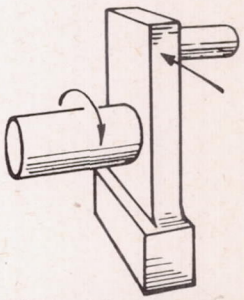

(c) Bending moment in plane of web.

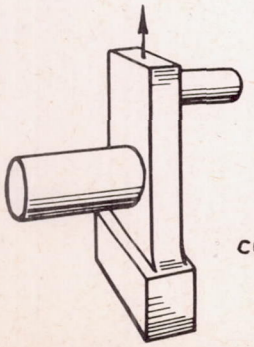

(d) Tensile-compressive force on web.

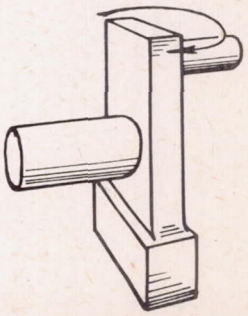

(e) Twisting moment on web.

Figure 6. - Forces and moments on crankshaft.

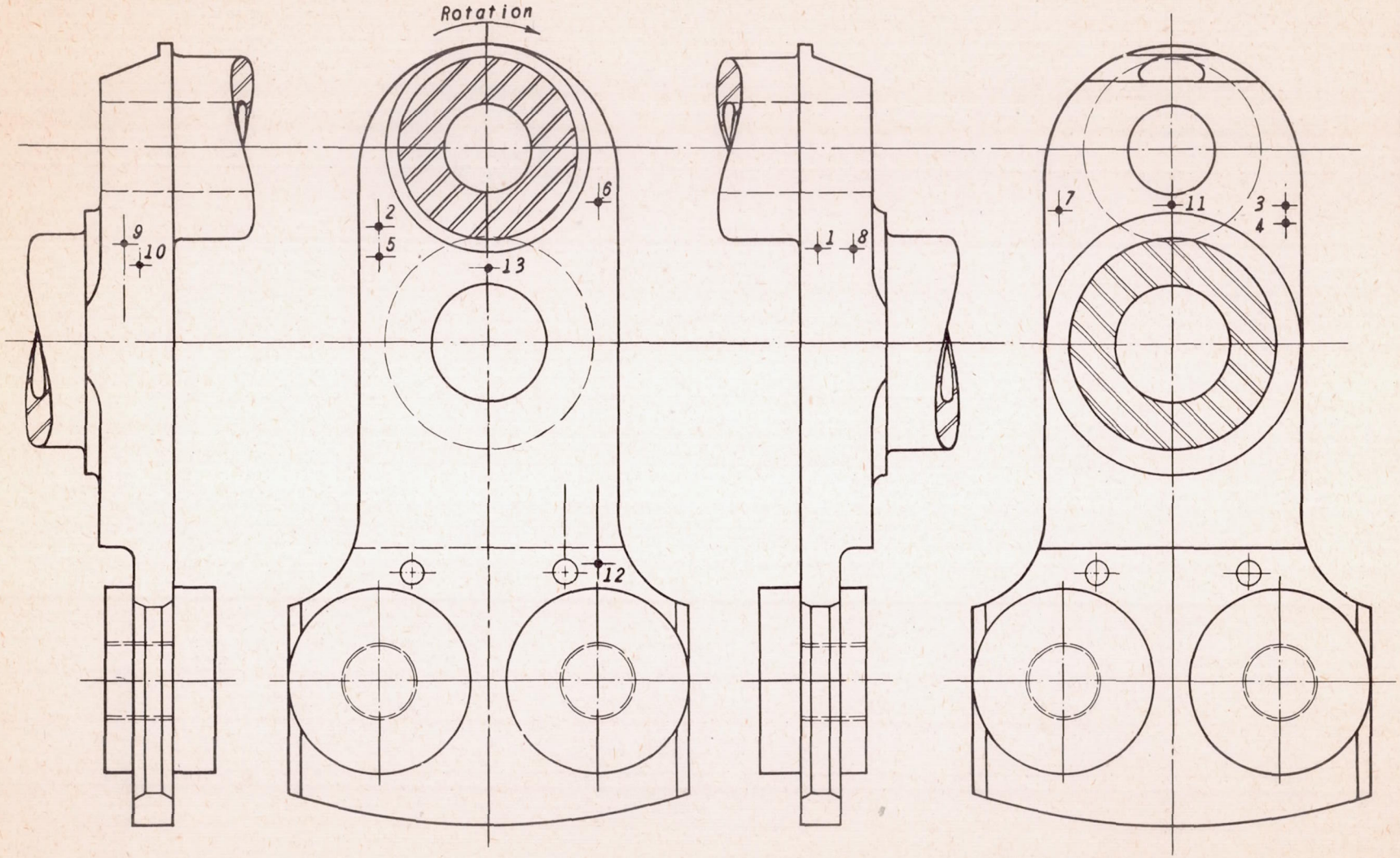

NATIONAL ADVISORY
COMMITTEE FOR AERONAUTICS

Figure 7. - Location of strain gages on crankshaft.

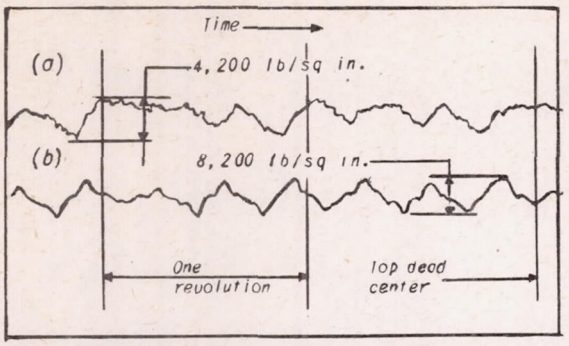

Figure 8. - Record taken with engine being motored. Engine speed, 2300 rpm; (a) gages 2 and 3, bending; (b) gages 4 and 5, tensile-compressive.

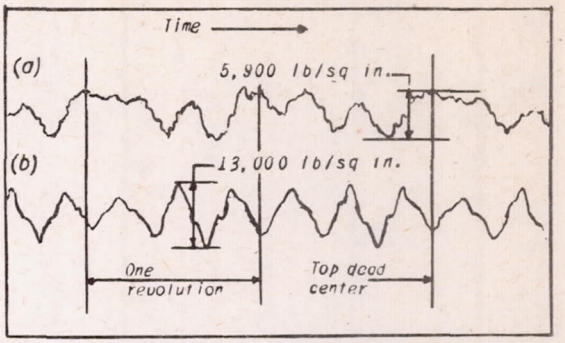

Figure 9. - Record taken with engine being motored. Engine speed, 2700 rpm; (a) gages 2 and 3, bending; (b) gages 4 and 5, tensile-compressive.

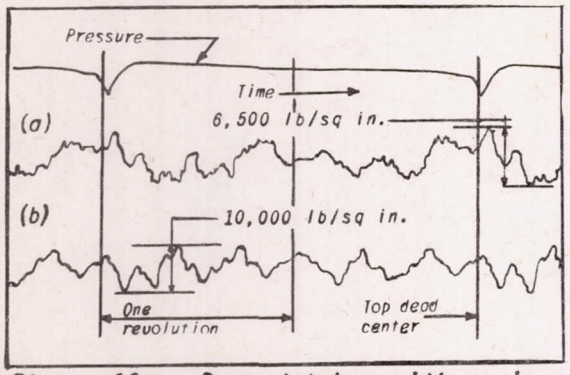

Figure 10. - Record taken with engine under power. Engine speed, 2300 rpm; manifold pressure, 30 inches mercury absolute; (a) gages 2 and 3, bending; (b) gages 4 and 5, tensile-compressive.

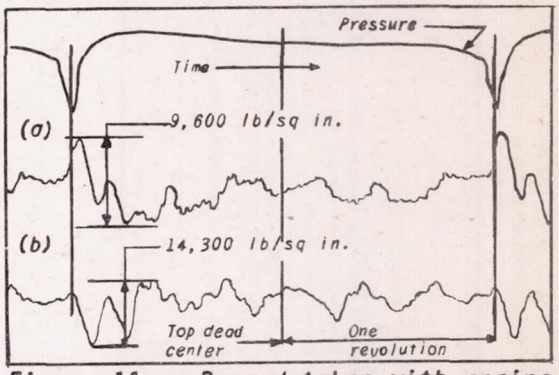

Figure 11. - Record taken with engine under power. Engine speed, 2300 rpm; manifold pressure, 49 inches mercury absolute; (a) gages 2 and 3, bending; (b) gages 4 and 5, tensile-compressive.

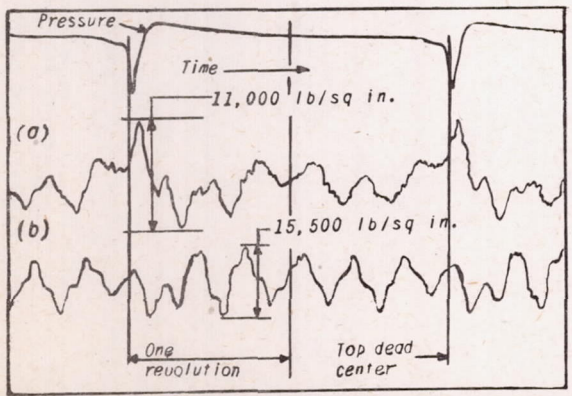

Figure 12. - Record taken with engine under power. Engine speed, 2700 rpm; manifold pressure, 40 inches mercury absolute; (a) gages 2 and 3, bending; (b) gages 4 and 5, tensile-compressive.

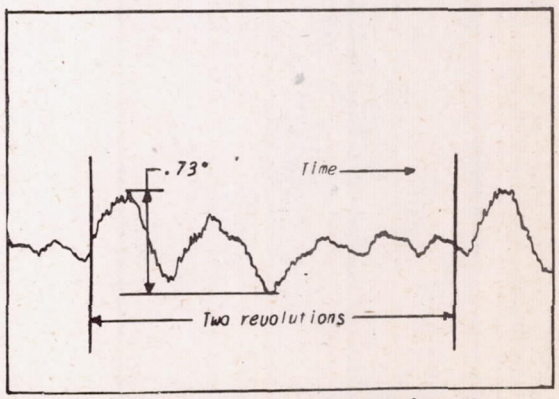

Figure 13. - Record of torsional vibrations taken with engine under power. Engine speed, 2300 rpm; manifold pressure, 40 inches mercury absolute.

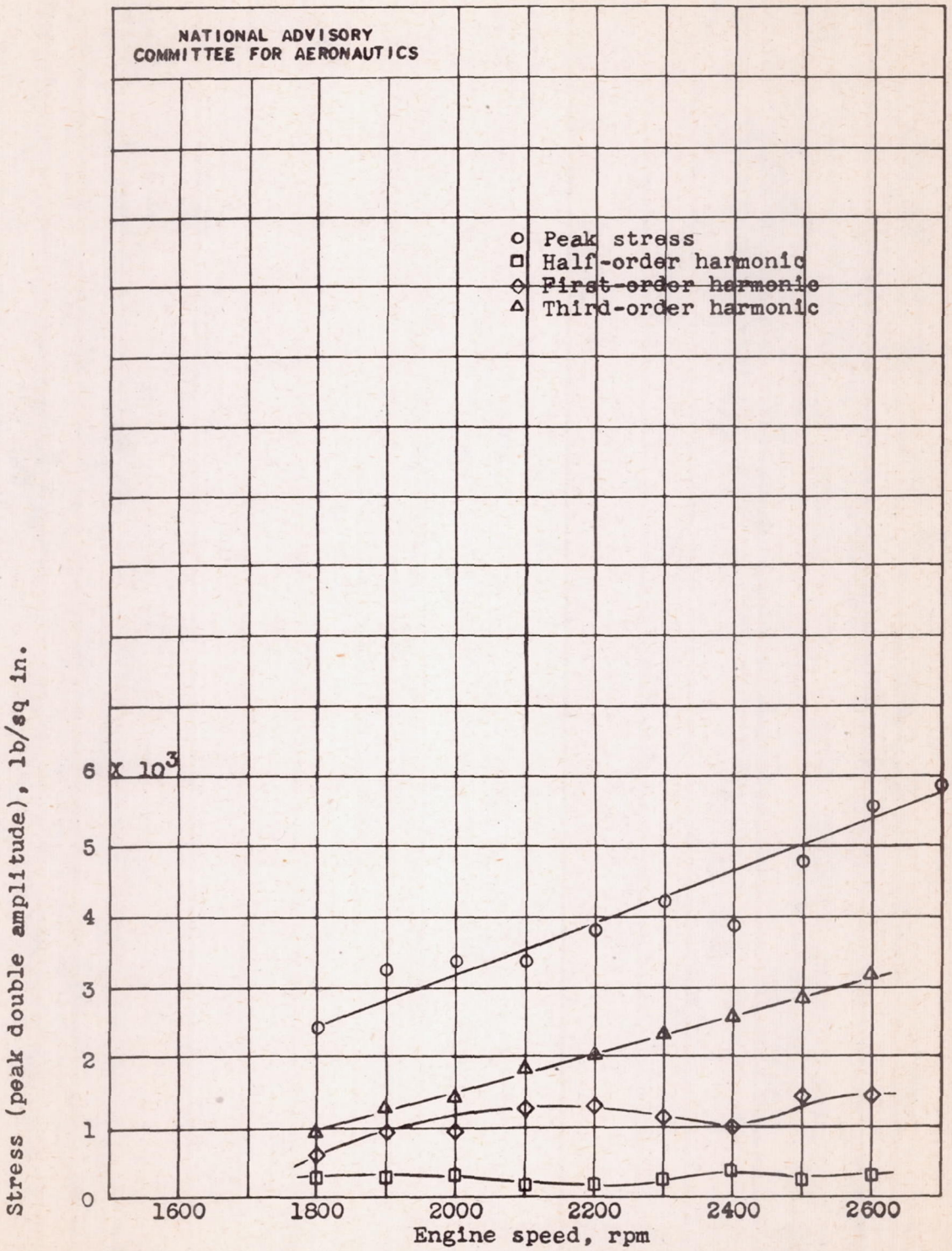

Figure 14.- Bending stresses caused by inertia forces with engine being motored. Gages 2 and 3.

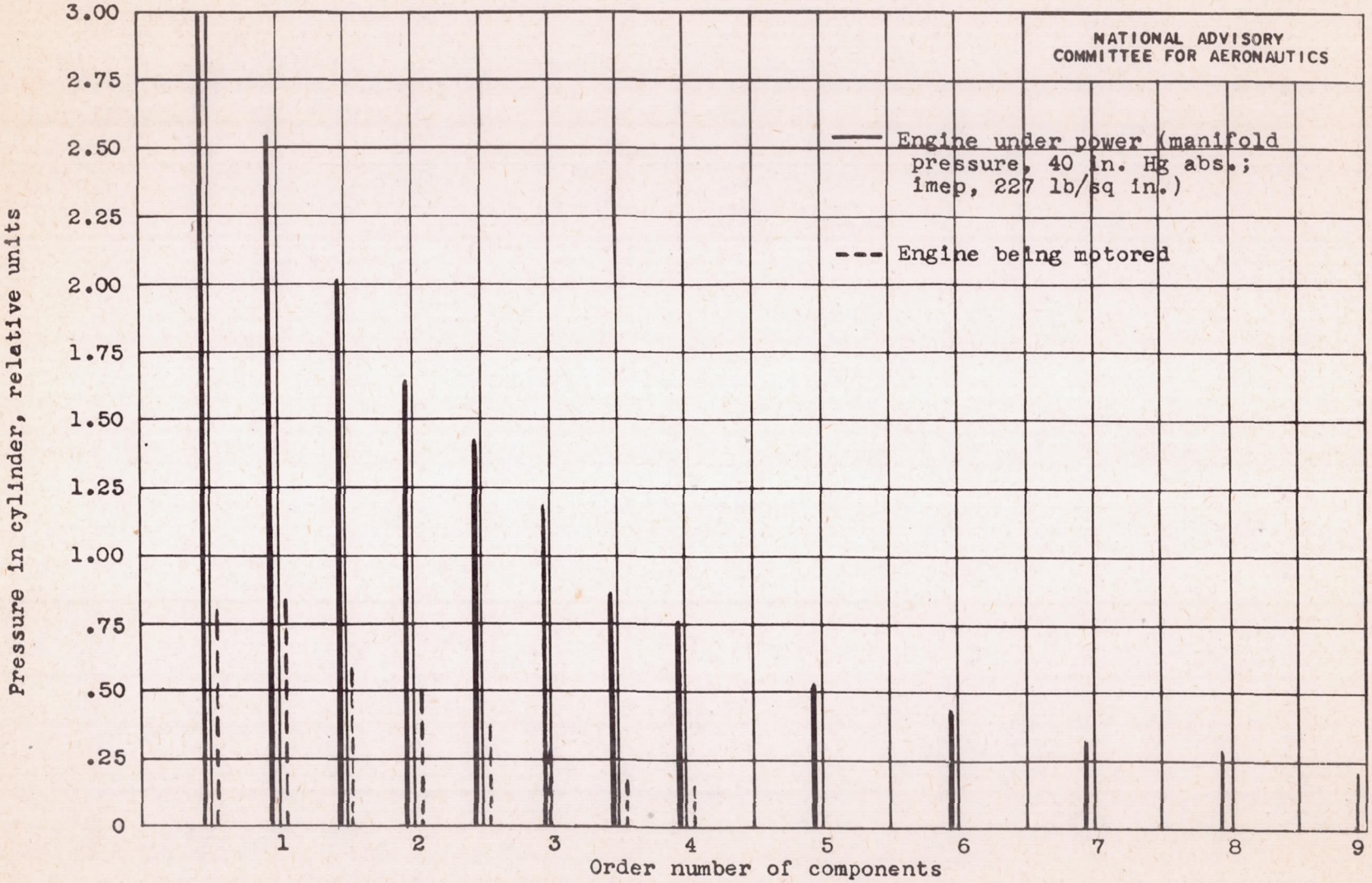

Figure 15.- Harmonic components of gas pressure in cylinder as measured by pressure indicator. Engine speed, 2300 rpm.

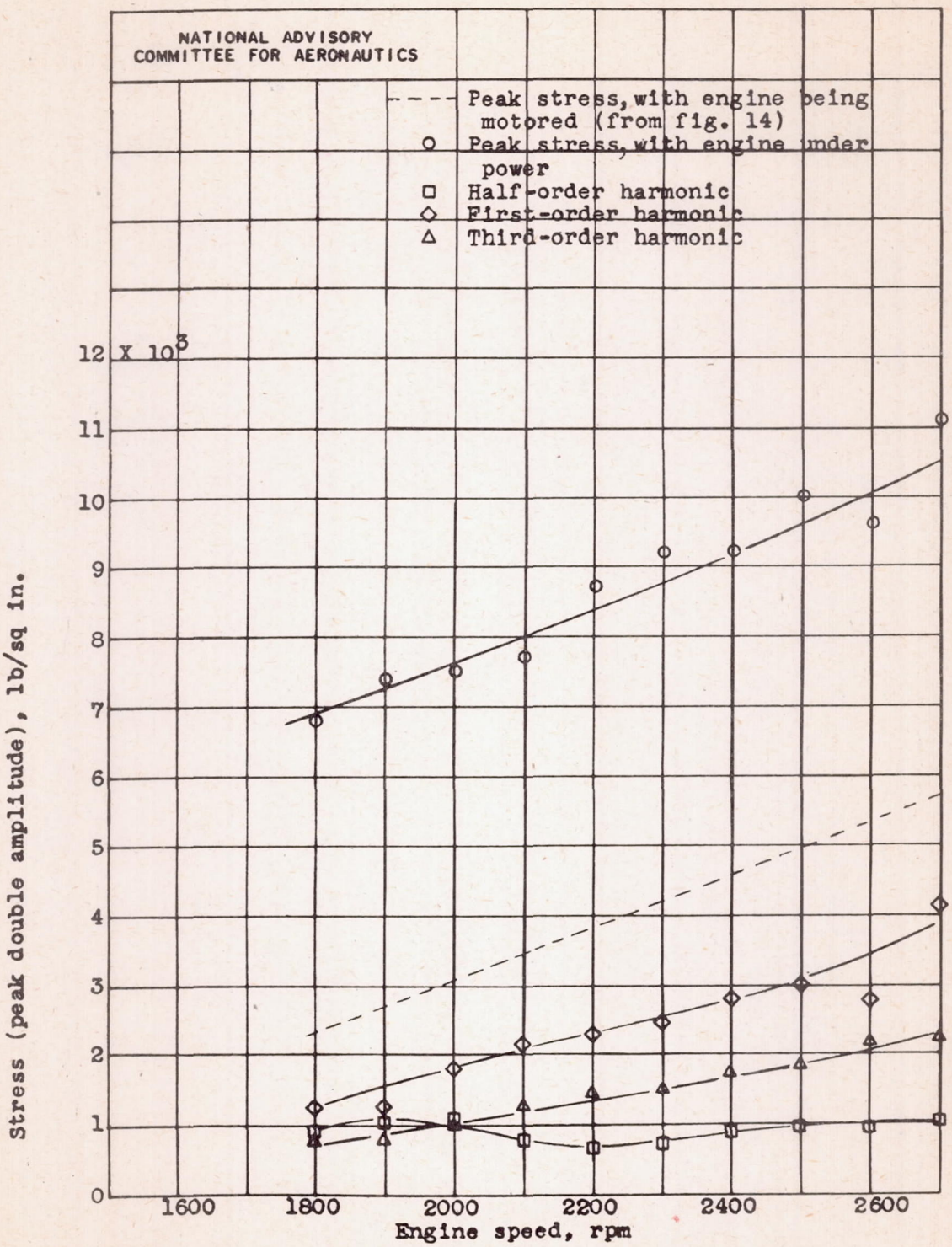

Figure 16.- Bending stresses with engine under power. Manifold pressure, 40 inches mercury absolute; gages 2 and 3.

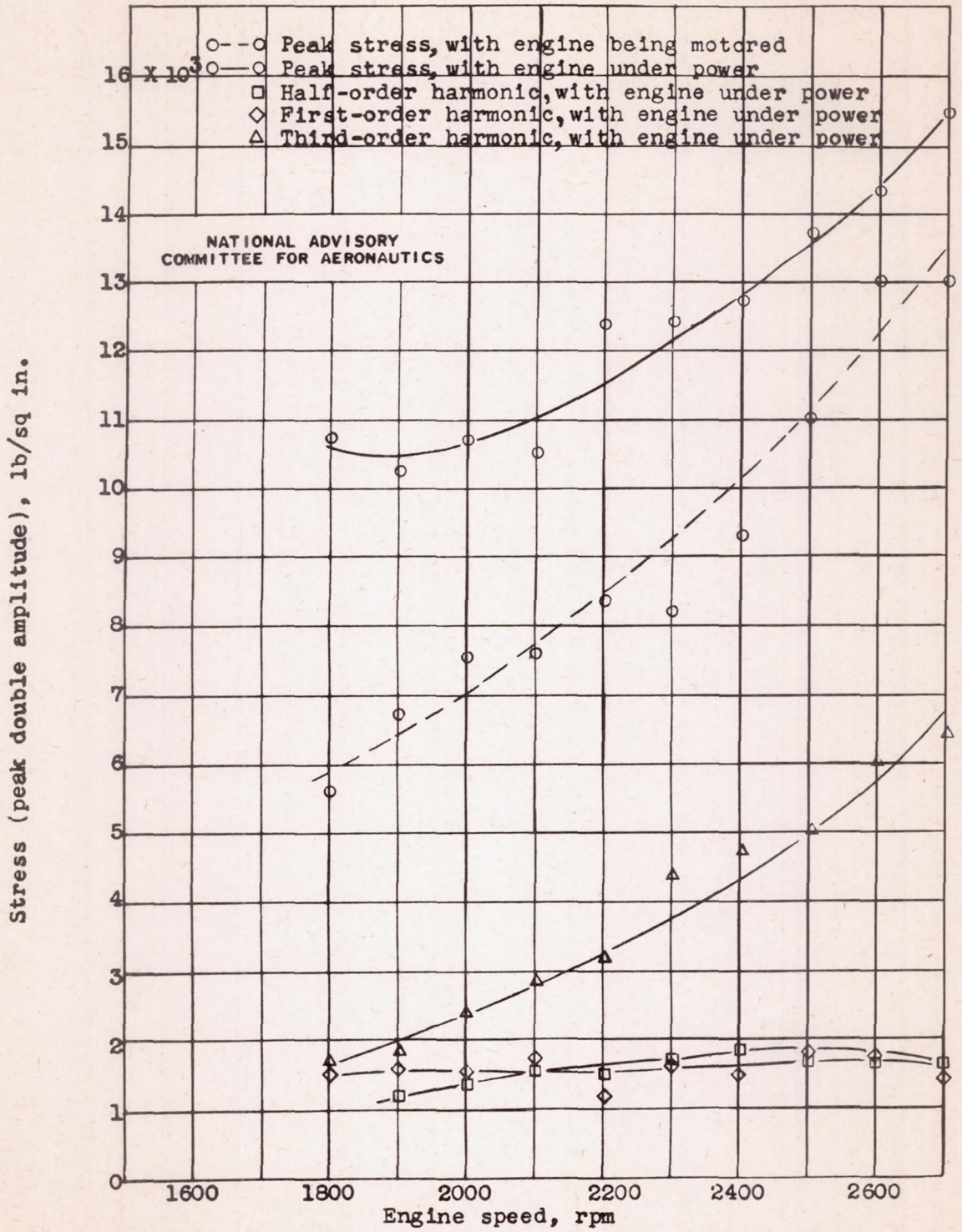

Figure 17.- Tensile-compressive stresses with engine being motored and under power. Manifold pressure, 40 inches mercury absolute; gages 4 and 5.

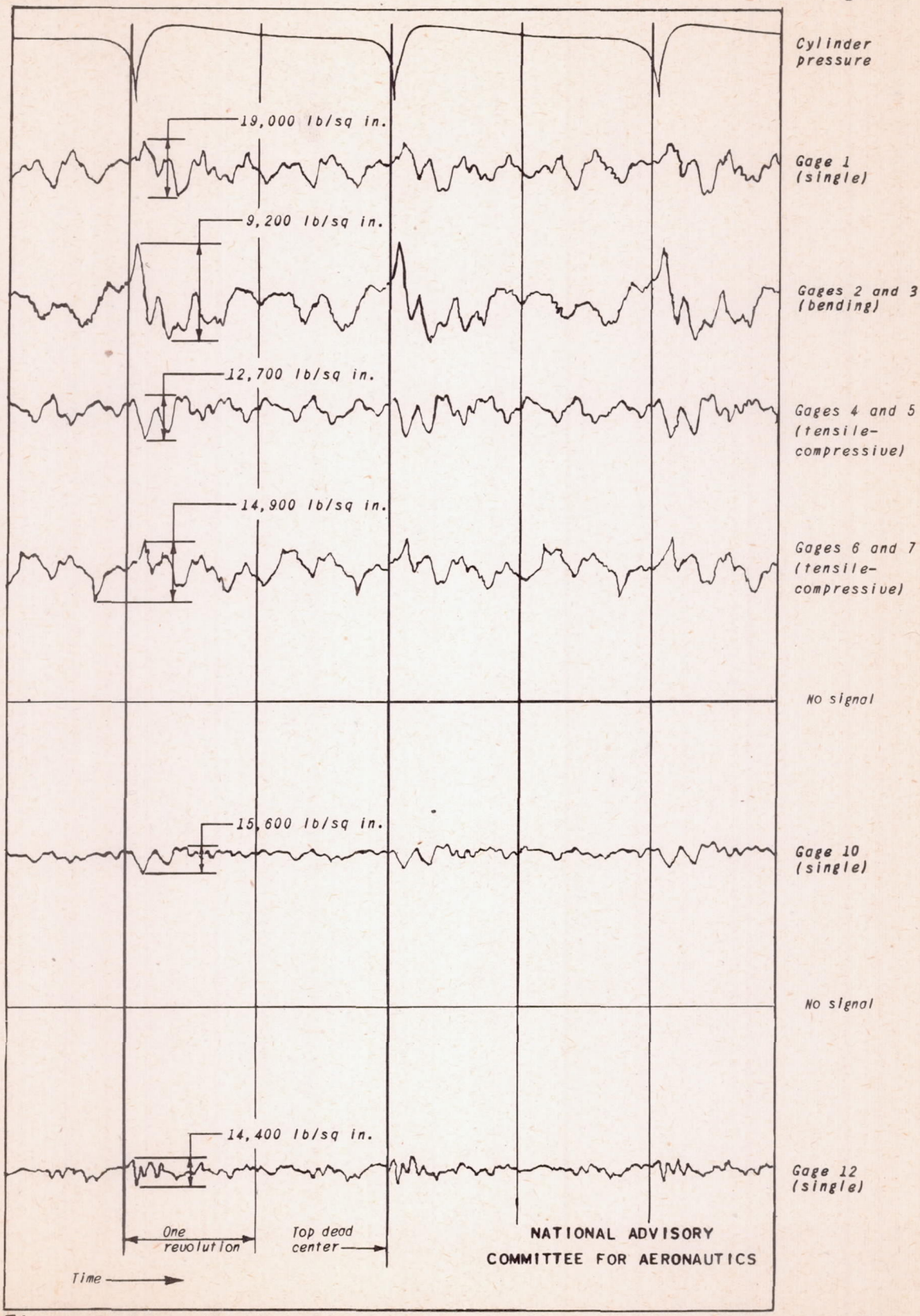

Figure 18. - Simultaneous record of several strain signals. Engine speed, 2400 rpm; manifold pressure, 40 inches mercury absolute.

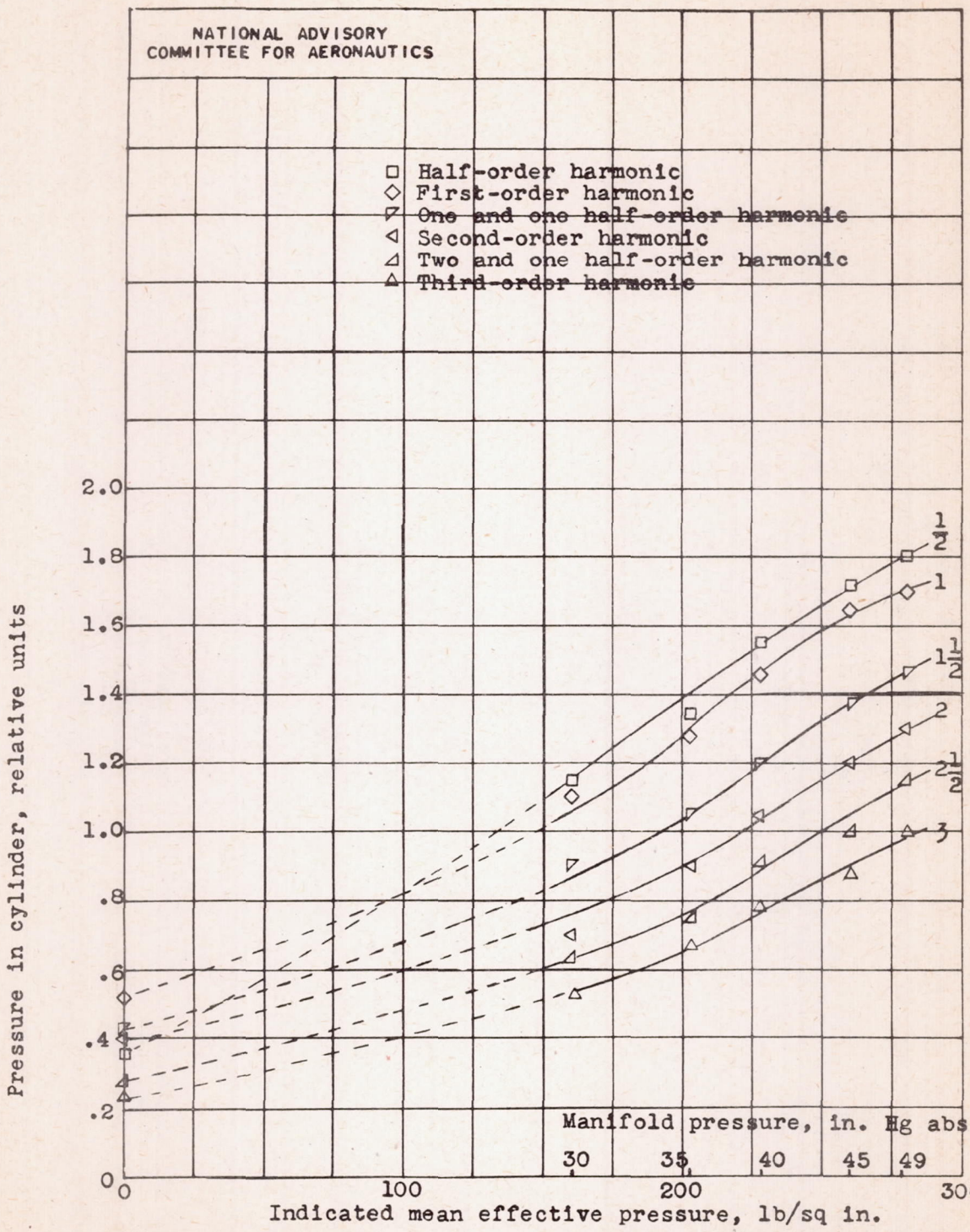

Figure 19.- Harmonic components of cylinder pressure at various manifold pressures. Engine speed, 2300 rpm; fuel-air ratio, 0.095.

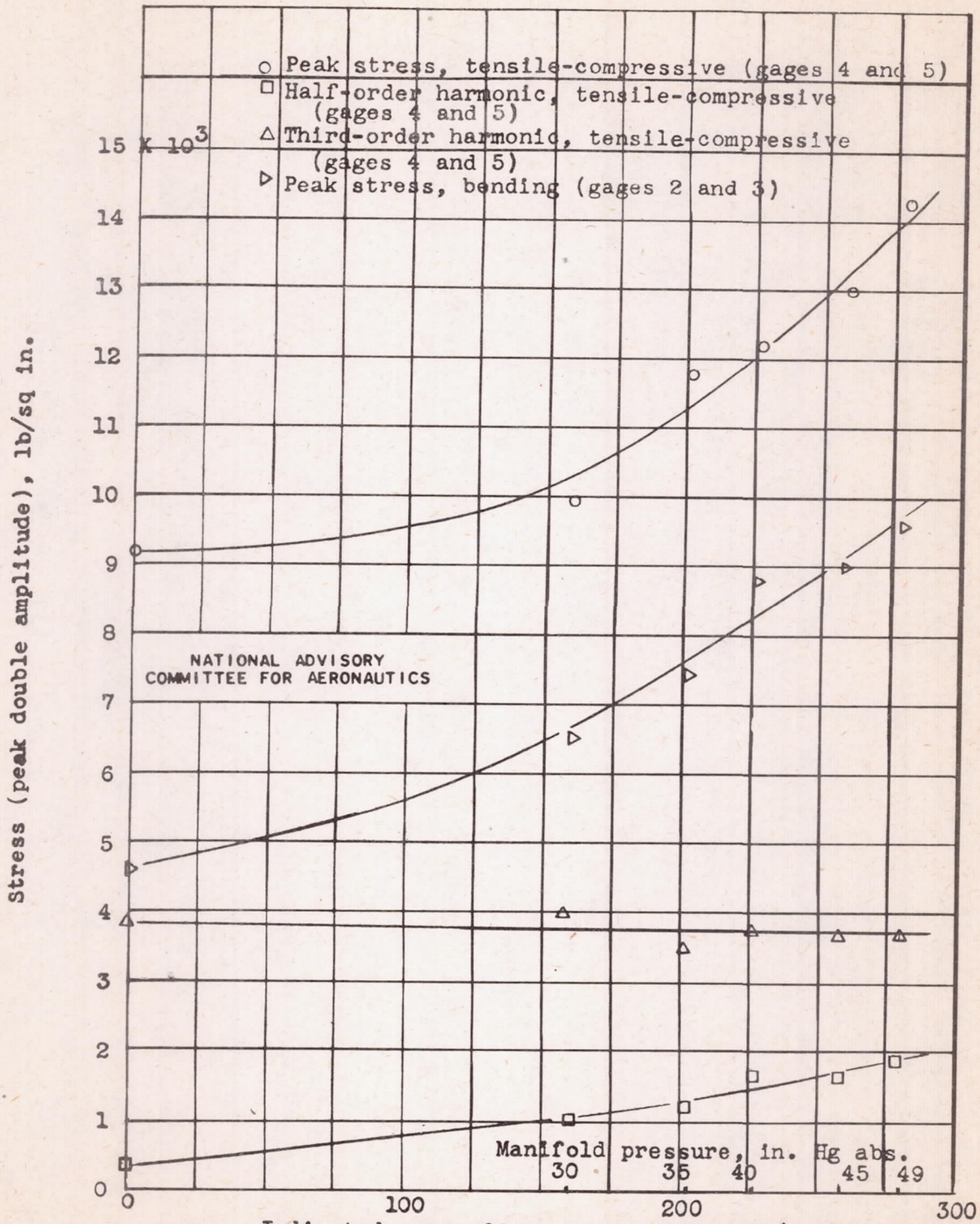

Figure 20.- Variation of stresses with manifold pressure. Engine speed, 2300 rpm; fuel-air ratio, 0.095.

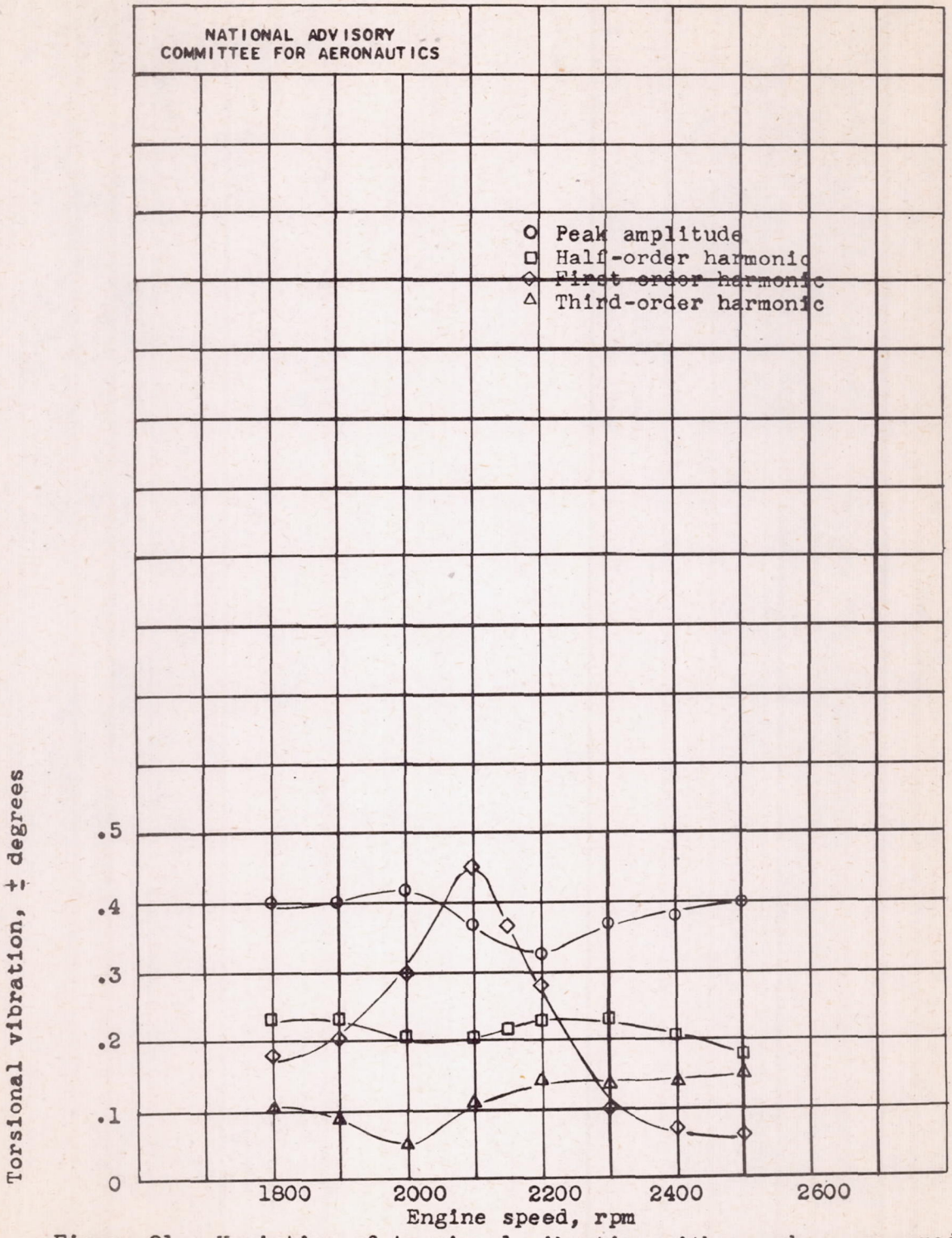

Figure 21.- Variation of torsional vibration with speed as measured with a torsiograph installed at the rear end of the crankshaft. Manifold pressure, 40 inches mercury absolute.